JAHANSHAHI, S., ZHANG, L., SUN, S., LANGBERG, D., XIE, D., and CHEN, C. Modelling physico-chemical properties of melts and kinetics of coal-slag reactions. *VII International Conference on Molten Slags Fluxes and Salts,* The South African Institute of Mining and Metallurgy, 2004.

Modelling physico-chemical properties of melts and kinetics of coal-slag reactions

S. JAHANSHAHI, L. ZHANG, S. SUN, D. LANGBERG, D. XIE, and C. CHEN
CSIRO Minerals, Clayton South, Victoria, Australia

An overview of recent development of CSIRO's Multi-Phase reaction models will be presented with examples comparing the calculated physico-chemical properties of metallurgical slags with the existing experimental data. The paper will also outline the development of a kinetically based model for molten bath reactors and its application to submerged combustion of coal in a slag bath as well as the reaction between the slag and injected coal particles. The plume model combines established models for the combustion of pulverized fuel with models for the growth and rise of bubbles from a lance or tuyere. This model predicts the extent of de-volatilization and combustion of the coal in the plume, the utilization of oxygen and the exchange rate of oxygen between the gas and the bath as well as the heat transfer rate between the gas bubbles and the bath. The slag reduction model brings together the recently measured rate data and fundamental understanding of the kinetics of CO-CO_2 reaction with iron oxide containing slags and predicts the changes resulting from injection of coal particles into molten slags. The top-space model covers reactions between gases and molten droplets in the post-combustion zone, where heat and mass transfer between phases results in higher utilization of the fuel values in the partly oxidized gases and transfer of heat to the molten bath.

Keywords: Phase equilibria, viscosity, electrical conductivity, slags, kinetics, reaction rate.

Introduction

The increased use of mathematical models in design and optimization of smelting and refining processes has led to a growing demand for sophisticated tools with capability to account for non-ideal behaviour of complex metallurgical melts and solid solutions. A large number of packages have been developed with capability of calculating the thermodynamic properties of multi-component high temperature phases. Most of these software packages have gained wide acceptance among the research and plant metallurgist communities and have led to development of improved understanding of smelting and refining processes as well as their metallurgical performance. The definitive work by Gaye and Welfringer[1] is a good example to draw upon, where application of the IRSID's cell model to inclusion engineering has led to a number of breakthroughs in production of high quality clean steel[2–3]. Their early work on the development of the cell model was presented about 20 years ago, at the second meeting of the present conference series, and outlined the potential capability of their thermodynamic model as a tool for process metallurgists. This was a very inspiring piece of work and motivated some of the Australian researchers and industry to look into broader application of the cell model.

At CSIRO work on development and application of slag models started in the early 90s as part of an R&D programme aimed at development of predictive models of metallurgical processes for the industry. The first phase of this work was focused on thermodynamic and transport properties of oxide melts and solid solutions, which included critical assessment of experimental data on both ferrous and non-ferrous systems of interest to the industry. This was then extended to include some molten salts and oxy-halide phases that are of interest to the aluminium industry and treatment of fluorine containing by-product wastes. As knowledge of the transport properties of metallurgical slags was limited, a series of targeted experimental studies was initiated in parallel to development of structurally related models of viscosity, diffusivity and conductivity of slags. The on-going work has resulted in development of CSIRO's MPE package that is now being widely used in Australia and South Africa.

The second phase of the on-going work at CSIRO involves kinetics of reactions between phases in smelting processes, with particular emphasis on coupling thermodynamic models of multi-phase reactions, with heat and mass transfer and interfacial reactions in bath smelting processes. This model attempts to account for various reactions taking place in molten bath reactors by drawing upon the wealth of fundamental knowledge and understanding developed over the past two decades on the physics and chemistry of coal injection into melts. Thus allowing simulation of reactions for de-volatilization and combustion of injected pulverized coal, growth and rise of bubbles from injection lance/tuyere, rate of oxygen exchange between phases as well as heat transfer rate between phases in different zones of the reactor, including the top space.

The present paper provides an overview of the recent development of the models at CSIRO with a few examples to demonstrate the current capability of our models by drawing parallels between the predicted behaviour and measurements from laboratory and plant based activities.

Thermodynamic modelling in high temperature metallurgical systems

Details of the thermodynamic models and methodology used in development of the CSIRO's MPE package are provided elsewhere[4–5]. In brief a number of solution models and associated databases are used for describing the thermodynamic behaviour of slag, alloy, matte and solid solutions of interest. The databases for the solution models have been developed using critically assessed and consistent experimental data on binary and ternary systems and validated against measurements on higher order systems. Through linking the solution models and databases with a free energy minimization routine, phase equilibria calculations are carried out. The cell model, which is used for calculating the thermodynamic behaviour of molten slags and salts, has an extensive database and allows description of simple and multi-component melts containing; SiO_2, Al_2O_3, Cr_2O_3, TiO_2, Ti_2O_3, Fe_2O_3, FeO, CaO, MgO, MnO, CrO, PbO, NiO, CoO, ZnO, Na_2O, Cu_2O, S and F. Other solution models used give descriptions of multi-component solid solutions (e.g. halite, spinel, corundum, olivine, pyroxene, melilite and psuedo-brookite), liquid alloys and matte.

In the following section of this paper a few examples of the predicted thermodynamic behaviour of metallurgical systems are used to illustrate their behaviour and make comparison with the measurements on some multi-component systems.

Liquidus temperature and stability of phases in SiO_2-MgO-FeO_x-CaO-Al_2O_3-CrO_x slags

Figure 1a shows the calculated phase boundaries for SiO_2-MgO-FeO_x based slags containing 10 wt% CaO, 5% Al_2O_3 and 2.5 % CrO_x at 1773 K and oxygen potential of 10^{-7} atm. According to this Figure, the liquid phase field is relatively small and fairly narrow composition ranges with respect to the MgO/FeO ratio. At higher MgO/FeO ratios, a spinel phase becomes stable as the primary solid phase. This spinel phase is rich CrO_x, MgO and FeO_x, with lower concentrations of Al_2O_3. Phase equilibria experiments carried out on industrial slags with comparable compositions (e.g Sample X) confirmed the stability of spinel ($[Cr,Mg,Fe,Al]_3O_4$) solid solution phase as the primary phase and the olivine ($[Mg,Fe,Cr]_2SiO_4$) solid solution phase as the secondary solid phase precipitating from the slags at temperatures below the liquidus. It is interesting to note that apart from the MgO/FeO ratio, the Cr_2O_3 content of these slags and its oxidation state had a strong influence on the stability of the spinel phase and hence the liquidus temperature. Figure 1b, illustrates the calculated effect of chromium content on the liquidus temperature and stability of other phases in the slag sample X, at oxygen potentials of 10^{-7} and 10^{-6} atm. For a given oxygen potential, the liquidus temperature increases sharply from about 1600 to about 1900 K as the chromium oxide content is increased from 0 to about 3 wt%, at higher chromium content the effect becomes milder. As shown on this Figure, the stability of the spinel also increases with increasing oxygen potential. Experimental data from a series of drop-quench tests on Sample X, showed the liquidus temperature of this industrial slag to be about 1900 K and at temperatures below 1700 K, the stable phases were spinel and olivine solid solutions in a matrix of glassy silicate. As shown in Figure 1b, these findings are in agreement with the calculated phase boundaries. It is interesting to note that the addition of most conventional fluxes tend to stabilize the spinel phase in this system. The above results outline a significant challenge facing the South African platinum industry with the increasing chrome in their ore/concentrate, which could have a strong effect on slag viscosity and recovery of valuable metals.

Distribution of cobalt between matte and slag

One of the recent enhancements to the MPE package has been the extension of its databases to include the behaviour of cobalt in the slag, solid solution and matte phases. Detailed descriptions of the assessment of cobalt containing

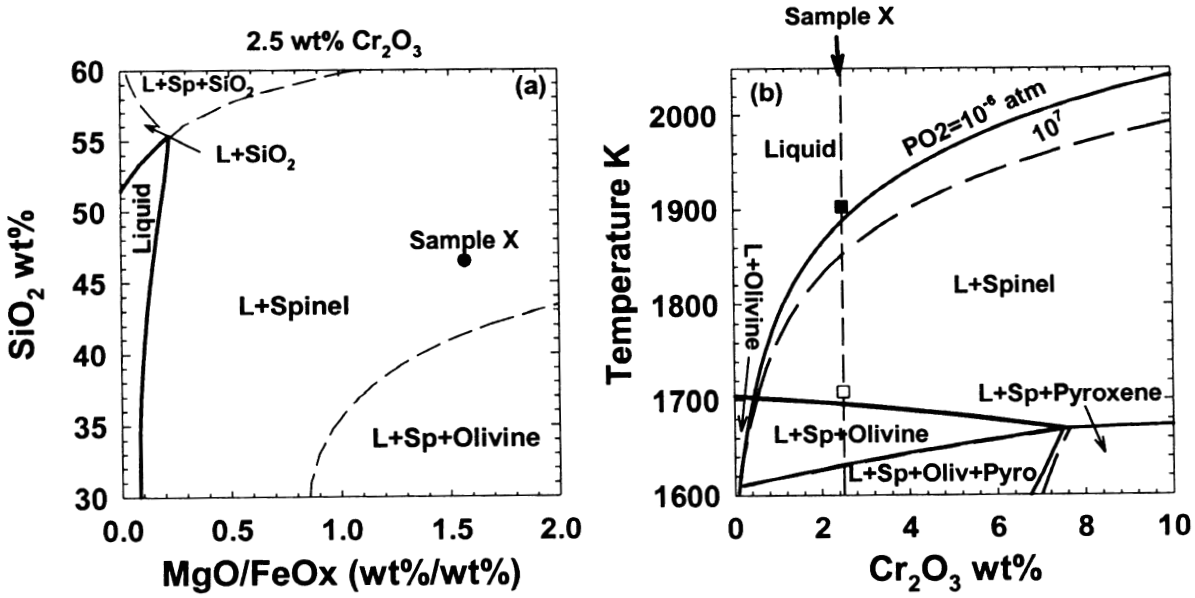

Figure 1. (a) The equilibrium phase regions in the CaO (10wt%)-MgO-FeOx-Al_2O_3 (5wt%)-SiO_2-Cr_2O_3 (2.5wt%) slag at $P_{O2} = 10^{-7}$ atm and 1773 K; (b) The effect of Cr_2O_3 and oxygen partial pressure on the equilibrium phase regions of the slag sample X as shown in (a). The symbol □ represents measured temperature when spinel phase started to precipitate out and symbol □ represents measured temperature when olivine phase started to precipitate out

systems have been provided elsewhere[6]. Recently the model was used to estimate the degree of departure from equilibrium between matte and slag in a number of industrial processes. In Figure 2, an example of such a comparison is presented, where the measured distributions in a number of processes[7–11] were found to be close to the calculated equilibrium values by the MPE package. It is interesting to note that for most cases, the measured distributions of cobalt between the matte and slag is less than the corresponding equilibrium distribution. This indicates that some improvements in cobalt recovery could be achieved by taking appropriate measures to reduce the degree of dis-equilibrium between the phases. Furthermore, studies on thermodynamics of cobalt in slags indicate that reduction in cobalt and copper losses to slags could be achieved by using slag modifiers.

Fluoride containing systems

The applicability of the cell model for describing the thermodynamic behaviour of molten salts used in aluminium smelting was presented at the 1997 meeting of this series of symposia. In that study[12] it was found that existing phase diagrams and activity data on binary, ternary and higher order fluoride systems could be well represented by using the cell model for the liquid phase and a solid solution model. Our more recent work has been looking into the behaviour of multi-component oxy-fluoride slags. In Figure 3 the predicted effect of NaF addition on the phase boundaries in Al_2O_3-CaO-FeO_x-MgO-SiO_2 slags at 1473 K is presented. These results show that addition of NaF has a marked effect on extending the liquid region by reducing the stability of melilite and spinel solid solutions, probably through reducing the activities of Al_2O_3 and SiO_2 in the liquid phase. While these predictions were found to be in accord with our experimental findings, further refinement of model parameters would be required to improve the accuracy of predictions over a broader composition range. Nevertheless, the agreement obtained illustrates the predictive capability of these thermodynamic models in regions with little or no pre-existing experimental data.

Modelling physical properties of slags

Compared to thermodynamic modelling of metallurgical slags, less progress has been made in modelling physical properties of slags. However, due to the important role of the slag properties on performance of processes there has been a growing interest in development of models of slag viscosity, conductivity, surface and interfacial tensions. In the present paper some highlights from our work on modelling of viscosity and electrical conductivity of metallurgical slags will be presented.

Viscosity of copper-nickel smelting slags

Details of a structurally related slag viscosity model developed at CSIRO were presented previously[13–14]. This model is capable of estimating viscosity of multi-component silicate melts from a knowledge of the behaviour of binary silicate melts. The model was later extended to account for the effect of suspended solid particles[15]. Recent experimental work on liquidus temperature and viscosity of some smelting and converting slags produced in South Africa has shown two orders of magnitude variation in the viscosity (0.2 to 20 Pa.s) with strong effects of slag chemistry and temperature. The slags with lower SiO_2 and Cr_2O_3 concentrations were more fluid, while slags with the lowest FeO_x and highest SiO_2 concentrations were the most viscous. These observations are in accord with general behaviour of silicate slags and the predictions of the viscosity model within MPE package. Phase equilibria studies on these slags had shown the stability of oxide solid solutions (spinel, olivine) in most of these industrial slags containing up to 3% Cr_2O_3, over the temperature range covered (1623 to 1823 K). In Figure 4, a comparison is made between these measurements[16] and the

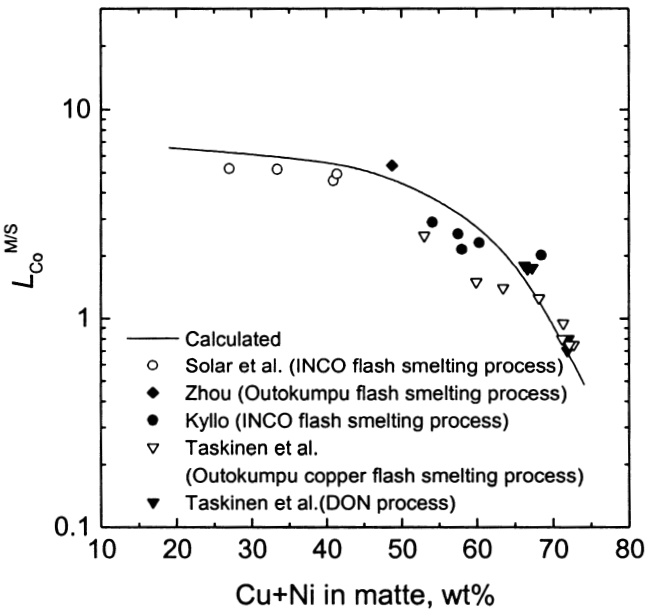

Figure 2. Comparison between calculated Co distribution coefficient ($L_{Co}^{M/S}$ = wt% Co in matte/wt% Co in slag) and measured data[7–11] from a number flash smelting processes

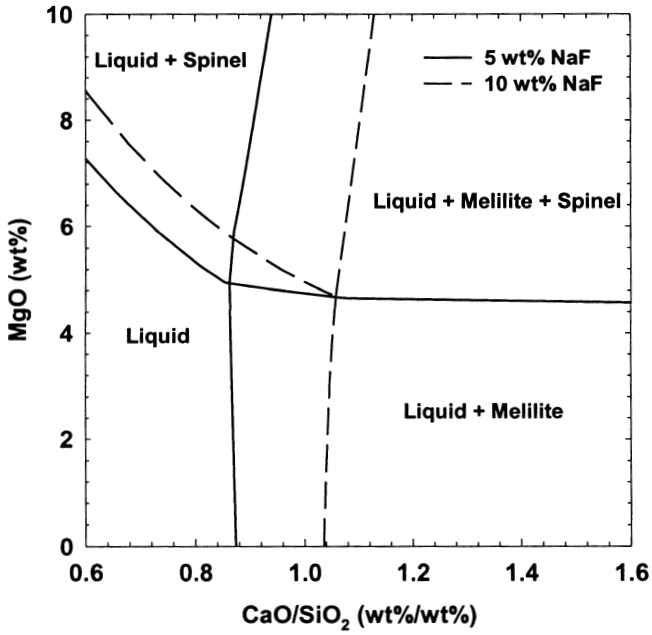

Figure 3. Model prediction of the effect of NaF (5 and 10 wt%) on the equilibrium phase regions in the NaF-CaO-Fe_2O_3 (10wt%)-Al_2O_3 (20 wt%)-MgO-SiO_2 slags at 1473 K

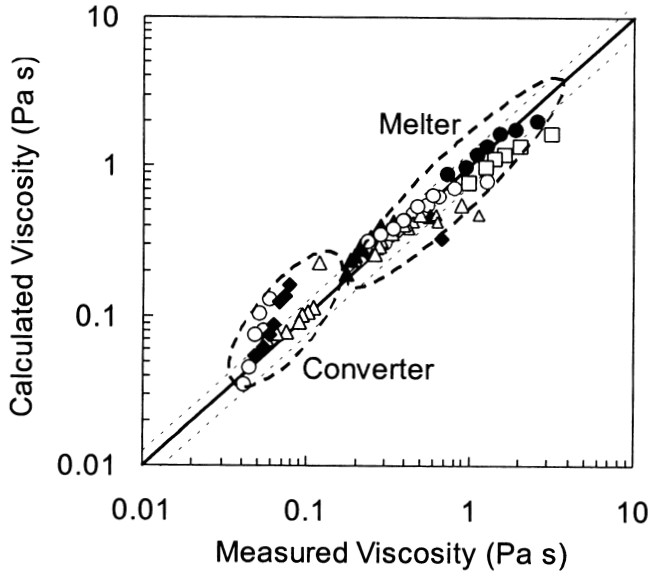

Figure 4. Comparison of the measured and calculated viscosity of slags from copper-nickel smelters and converters in South Africa

calculated viscosity according to the MPE model. This Figure illustrates that when the calculated effect of solid phases is taken into account, the difference between the measured and calculated viscosity of these complex slags is mostly within the typical uncertainty in the experimental values (±30%). There are, however, a few measurements on the converter slags that show lower viscosity than the corresponding calculated values. This is likely to be due to errors in the calculated liquidus temperature and/or chemical analysis of slags with respect to Fe^{3+} and Fe^{2+} concentrations.

Viscosity of coal ash slags

Coal ash slags are generally richer in Al_2O_3 and SiO_2 than metallurgical slags with variable FeO_x and CaO contents. In some cases use is made of fluxes such as CaO and FeO_x to reduce the viscosity of the coal ash slag to below 25 Pa.s for smooth tapping of slag at operating temperatures of 1673 to 1773 K[17]. Reliable viscosity models can serve as a useful tool for the industry in development of guidelines for blending different types of coal and fluxing practice for smoother operation of the gasifiers. This opportunity was explored by first validating the MPE package against comprehensive sets of experimental data obtained by Hurst *et al*.[18–19] on synthetic slags and fluxed coal ash slags. This comparison showed good agreement between the measured and predicted viscosity of slags over three orders of magnitude (0.2 to 162 Pa.s).

With such high levels of confidence in the model, its application to assessing suitability of Australian bituminous coals for power generation using the IGCC (integrated gasification combined cycle) process was illustrated through construction of operating diagrams[20] such as the one shown in Figure 5. In this Figure the variation of viscosity with composition of coal ash slags containing 15 wt% FeO_x at 1723 K is shown in the form of iso-viscosity contours. Measured viscosity data by Hurst *et al*., and the stability region for the anorthite ($CaAl_2Si_2O_8$)[21] outlined by the shaded area are also shown on the Figure. As can be seen, for a given CaO content, the viscosity increases with increasing SiO_2/Al_2O_3 ratio. This increase in viscosity becomes less pronounced at high CaO content. The calculated viscosity values in the shaded area, where the solid anorthite phase is stable, are extrapolations of liquid viscosity and are expected to be less than the experimental data if crystallization occurs. These calculated values in the two-phase region are not very far from the experimental data, thus suggesting that either these slags were supercooled or that a small concentration of anorthite particles does not have a significant effect on the viscosity of these slags.

As mentioned previously, experience in operating these gasifiers indicates that for smooth operation and slag tapping the viscosity of slags should be less than 25 Pa.s. Thus according to Figure 5, the CaO content of the slag needs to be about 5 wt % for SiO_2/Al_2O_3 ratio of 2.4. At lower SiO_2/Al_2O_3 ratios in the slag, higher levels of CaO could be used to avoid formation of the anorthite phase.

Electrical conductivity of melter type slags

Electrical conductivity of slags has been the subject of some investigations and our knowledge and understanding of this property of metallurgical slags has improved over the past decade or two. Most of the published data on conductivity of simple and complex slags have been compiled and reviewed by Mills[21]. The published data on slags show about four orders of magnitude increase in the conductivity as the FeO_x content increases from 0 to 100%. Unlike viscosity of slags, electrical conductivity tends to increase with increasing temperature and slag 'basicity'.

Recent work by Hundermark[22] on electrical conductivity of melter type slags (SiO_2-MgO-FeO_x-Al_2O_3-CaO) with and without Cr_2O_3 addition has provided new data on types of slags produced by electric smelting of copper-nickel concentrates in South Africa. In Figure 6 some of the results obtained by Hundermark are presented. These results show variations in conductivity of slags with 30%

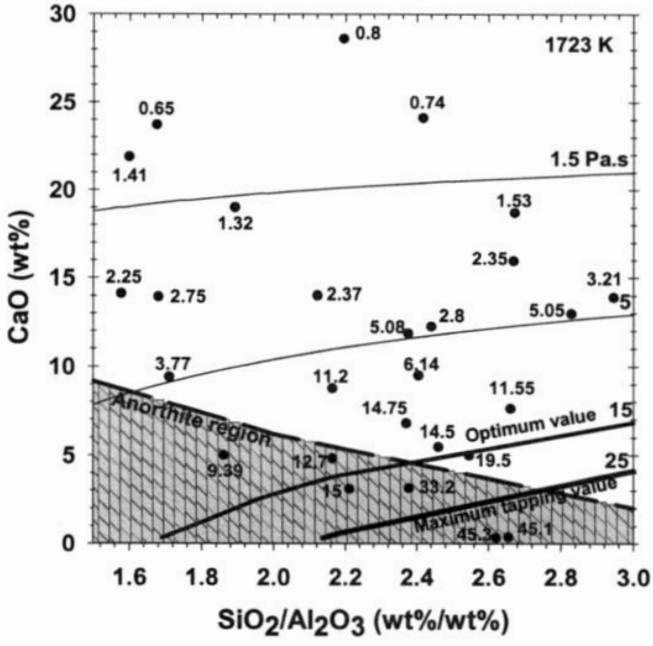

Figure 5. Viscosity variation with amount of CaO flux and SiO_2/Al_2O_3 ratio at 15wt% of 'FeO' and 1723 K in the 'FeO'-CaO-Al_2O_3-SiO_2 based coal ash slags. Solid lines are calculated iso-viscosity curves and numbers are the experimental data of Hurst *et. al*.[17–19]

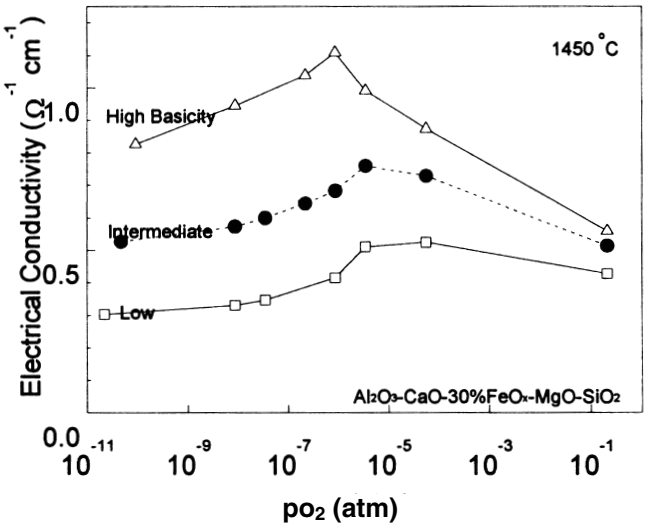

Figure 6. Variation of electrical conductivity of Al_2O_3-CaO-30%FeO_x-MgO-SiO_2 slags with basicity and oxidation state at 1623 K[26]

FeO_x with oxygen partial pressure for three levels of basicity at 1723 K. The effect of slag basicity on the conductivity is quite pronounced with conductivity increasing as the basicity increases. For a given slag basicity, the conductivity goes through a maximum at some intermediate level of oxygen partial pressure between air and iron saturation. The dependence of conductivity on the concentration and oxidation state of iron oxide could be attributed to the two roles that such transition metals could play. As a 'basic' oxide they can contribute towards depolymerzation of silicate melts and, therefore, could enhance mobility of cations as charge carriers. Their second role would be by enhancing charge transfer in the melt through processes involving Fe^{2+}, Fe^{3+} and electrons. This latter role could be termed as electronic conduction while the former role is ionic conduction. It follows that the observed maxima in conductivity of slags is an indication of the combined effects of the ionic and electronic conductions as the Fe^{3+}/Fe^{2+} ratio changes with oxygen potential.

There have been a number of models proposed for representing the composition dependence of conductivity of slags[23–25]. Most of these models give a good representation of the data over the limited composition range of the data used. A recent attempt[26] in modelling the behaviour of simple and complex slags over broad ranges of temperature and composition has shown very promising results of the type shown in Figure 7. This model gives close prediction of the conductivity over four orders of magnitude covering a temperature range of 1573 to 2023 K. The effect of Cr_2O_3 in such slags was also examined with good fit for slags with up to 8 wt% CrO_x, where newly measured experimental data exists.

Modelling of bath smelters

The last two decades have seen tremendous development of the bath smelting technology. The focus in the early days was on development of intensive bath smelting processes for production of base metals and, later, for finding alternative iron making processes to eventually replace the iron blast furnace route. Bath smelting technologies have turned out to be more flexible and versatile than just a replacement for the more mature technologies. They have found more applications in secondary smelting of non-ferrous materials including base metals and PGM smelting as well as in waste treatment. The development and commercialization of the SIROSMELT, Isasmelt and Ausmelt technologies took at least two decades and, today, over 3 M tpa of sulphide concentrates and mattes are being processed in such reactors around the world. A new addition to these bath smelting processes is the HIsmelt process that is designed for production of pig iron from iron ores and iron rich wastes. A 0.8 Mt/a pig iron HIsmelt plant is being constructed in Western Australia.

The wide application of the technology poses a range of issues regarding feed characterization, process chemistry, refractory wear, energy efficiency, heat utilization, process control etc. For the development, optimization and the control of the bath smelting processes, a computer model could be a handy tool. The authors have recently embarked on such an endeavour.

These smelter furnaces may be conceptually divided into three reactive zones: a 'plume zone' where gas and fuel/feed/reductant are injected, the bath zone and the top space where gaseous and gas-splash reactions continue. Accordingly, the model is constructed to include three modules corresponding to these three zones. The following sections outline the model using the coal reduction of iron oxide as an example. In the plume model, the combustion of coal particles in the gas bubble was modelled. The bath model considers the reaction between coal/char particles and the bath through the gas intermediate. The third part models the post combustion and the oxidation of the metal and slag splash by the gas and the heat transfer in the top space of the furnace.

Modelling the plume-coal combustion

In smelting reactors where the process heat is provided by submerged combustion (eg slag fumers, SIROSMELT-type vessels), the fuel (usually coal) and oxidant (air or oxygen) are injected beneath the bath surface from a lance or tuyere.

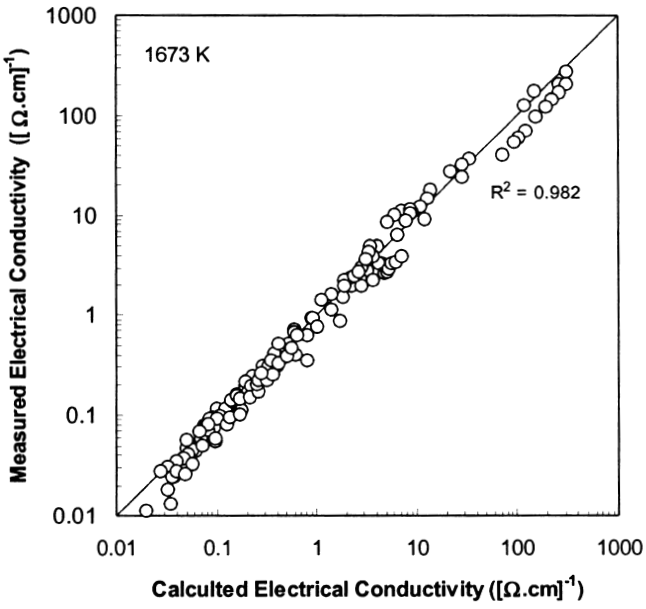

Figure 7. Comparison of measured and calculated electrical conductivity[26] for binary, ternary and higher order slags containing Al_2O_3, CaO, FeOx, MgO, SiO_2 at 1673 K

The primary combustion reactions occur in the plume of rising bubbles between the injector nozzle, and the bath surface. Efficient combustion of the coal in the bath is essential, for about half of the coal consumed in some smelting processes may be needed to provide the process heat[27]. Submerged combustion provides intimate contacting between the bath and the combustion mixture, which enables high heat transfer efficiencies to be attained. However, the residence times available for combustion in the plumes are short. Kinetic modelling of coal combustion in the plume will enable the coal properties and particle sizes, and injection parameters to be selected to maximize the extent of combustion during submerged combustion.

The plume model combines a kinetic model for the de-volatilization and combustion of pulverized fuels with a model for the growth and rise of bubbles from a submerged lance or tuyere. Validation is carried out by comparison of the model predictions with the published data, laboratory measurements and measurements from the SIROSMELT pilot plant at CSIRO Minerals' Clayton Laboratory.

The key phenomena which are modelled are:

- The separation, in the primary bubble formed at the injector nozzle, of the 'combustion' coal, which burns in the plume from the 'reduction' coal, which penetrates into the bath to reduce the slag
- The formation of the bubbles at the injector nozzle, and their subsequent rise to the bath surface
- The de-volatilization of the injected coal particles, and the combustion of the volatiles and char in the bubbles
- The transfer of heat between the combustion mixture in the bubbles, and the bath by convection and radiation
- The transfer of oxygen between the bubbles and the bath, and the extent of re-oxidation of the bath by the plume.

Examples of the behaviour predicted by the model are shown in the following figures. In this example, the submerged combustion of a bituminous coal containing 36% volatiles and 15% ash was modelled. The coal injection was assumed to be at a rate of 0.012 kg/s, through a tuyere located 1 m beneath the surface of a slag bath at 1473 K. The average particle size was 20 μm. Air (21 vol. % O_2) preheated to 900 K was injected at a rate of 3.76 mole/s to burn the coal. The initial coal particle temperature was assumed to be 300 K. The bubble formation and rise model predicted the bubble to detach after 0.25 s, and reach the bath surface after 0.4 s. The de-volatilisation and char combustion histories are shown in Figure 8. De-volatilization was relatively rapid, and was complete before the bubble surfaced. The char combustion was slower, and the conversion reached over 90% at the time of the bubble's surfacing. The unburnt char, due to small particle sizes, would easily be entrained by the combustion gases into the top space of the reactor.

The O_2, H_2O, and CO_2 concentrations are shown as functions of time in Figure 9. The oxygen concentration decreases slowly at first, until the particles heat and start to burn. The H_2O concentration stabilizes after bubble detachment, when the coal (and hence the volatiles) supply to the bubble ceases. The CO_2 concentration continues to rise as char combustion proceeds. The particle temperature is shown in Figure 8. The particle and gas temperatures were calculated to be almost identical for particles of this size. After a brief initial heating period of about 10 ms, the particle temperature peaked soon after it exceeded the bath temperature. It declined thereafter, when the heat generated by the slowing char combustion reaction was no longer able to match the heat transferred to the bath.

Modelling the smelter bath reactions-coal-slag particle reaction

A common feature of reactions between slags and injected coal or char particles is the existence of gas bubbles encapsulating the particle, with the gas facilitating the transfer of oxygen as illustrated in Figure 10. Taking iron bath smelting as an example, the overall reaction

$$C + (FeO)_{slag} = CO + [Fe]_{metal} \quad [1]$$

proceeds through the following consecutive reactions:

$$(FeO)_{slag} + CO = [Fe]_{metal} + CO_2 \quad [2]$$

at gas slag interface

$$CO_2(g) + C = 2CO(g) \quad [3]$$

at char surface

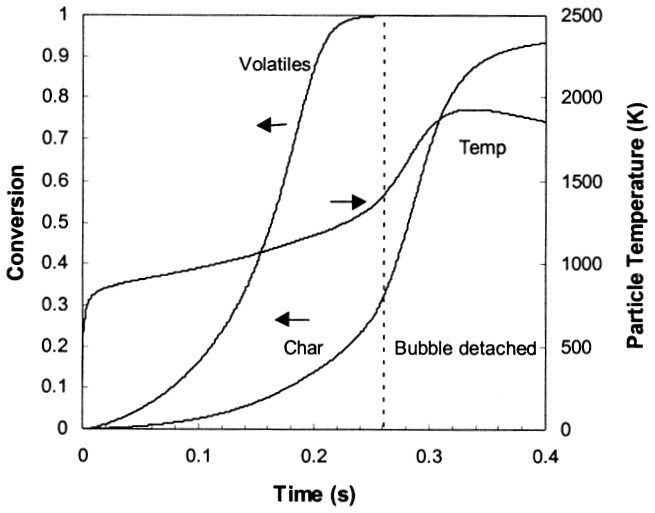

Figure 8. Variation of the extent of coal de-volatilization, char combustion and particle temperature with time in the plume. Dashed line showing time for bubble detachment

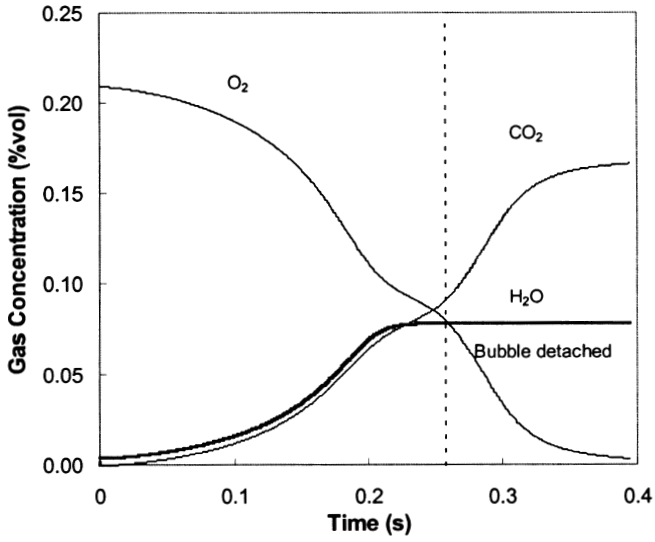

Figure 9. Gas composition in the bubble vs time. (Balance N_2)

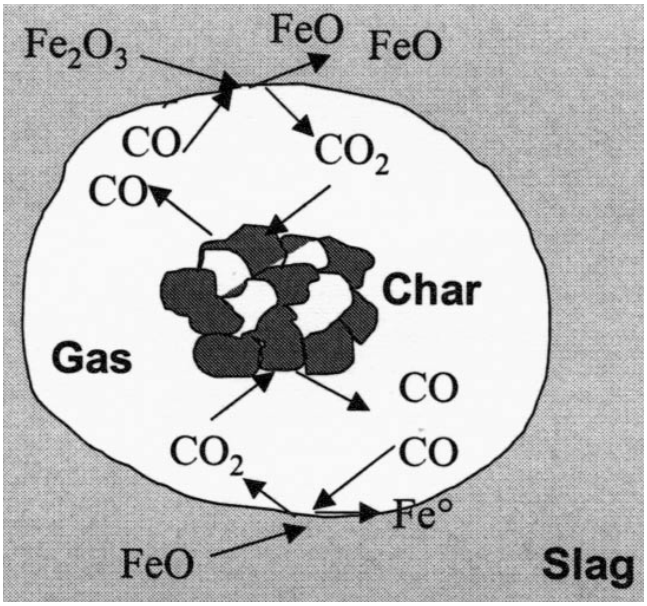

Figure 10. Schematic illustration of coal particle-slag reaction

The process may involve a series of steps: slag phase mass transfer, gas-slag interfacial reaction, and gas phase mass transfer and gas-char reaction.

Kinetics of coal-slag reactions has been the subject of extensive research efforts for a long time. Recently, Fruehan and co-workers[28–29] studied the kinetics of coal-slag reactions between a rotating rod (graphite or coke) and a slag bath with slag composition and temperatures pertinent to those used in bath smelting processes. The surface of the graphite rod was found to be covered by gas bubbles, hence the rates were dictated by similar slag-gas-char mechanisms to that for a coal particle injected into a slag bath (but apparently under different geometric conditions). Rates of gas-coal/char reactions with impinging CO-CO_2 and H_2-H_2O gases[30] were measured at 1573–1773 K. A mixed control model[31] was developed for slag-gas-coal reactions and general equations for sequential steps involving mass transfer and interfacial rates were derived. Model predictions agreed well with the observed overall rates which were, in general, controlled by various steps in a series. The gas-carbon reactions were found to have a significant effect on the overall rate for a coke rod.

In principle, the mixed control model by Fruehan *et al.* may also be applicable to the slag-coal particle reactions when the appropriate geometric conditions and relevant flow and mass transfer rates for a particle/bubble reaction cell are used. Mass balance, geometric condition, and mass transfer in particle/bubble cells[32] relevant to slag-coal particle reactions have been discussed in detail by Richards and Brimacombe[33] for the zinc fuming process. Based on these, a kinetic model for slag-coal particle reactions in bath smelting processes (for iron ore or similar smelting process) is being developed at CSIRO. The model and preliminary considerations of a few key issues are briefly discussed.

When coal particles are injected into slag bath at high velocity without sufficient preheating, coal devolatilization takes place mainly after the particles enter the slag bath. The coal devolatilization (usually much faster relative to the gas-char reactions) provides an initial gas bubble (of mainly H_2 and CO) surrounding the coal particle. For an average of 20% volatiles in the coal, the devolatilization can produce an initial gas mixture of volume close to about 40% of the final gas volume at complete reaction of the coal particle. The presence of hydrogen also means that reactions involving H_2-H_2O will take place in the particle-bubble cell. For these reasons, the reaction kinetics will differ considerably from the case when coke is used. The role of the volatiles and the H_2-H_2O reaction are two of the additional factors to be incorporated in the bath smelting model.

Reduction of ferric to ferrous iron may be involved when a feed high in Fe_2O_3 is used. The reaction sequence for iron oxide is $Fe_2O_3 \rightarrow FeO \rightarrow Fe$. It is conceivable that reductions of ferric to ferrous iron or ferrous to metallic iron will dominate in oxidized or reduced slags, respectively. At the intermediate stage, the two reactions may take place simultaneously. This could be modelled based on the 'oxygen' associated with iron for both slag mass transfer and interfacial reactions.

CO_2 (and H_2O) in the gas bubble plays a key role in linking the two interfacial reactions at the gas-slag and the gas-carbon interfaces. For the gas-slag reaction to proceed to reduce ferrous iron to metallic iron, the gas composition must be sufficiently reducing (low in CO_2 and H_2O). This will dictate not only the gas mass transfer rates within the bubble, but also the rates of gas-carbon reactions at the coal particle surface (as CO_2 is required to oxidize the coal to produce CO), particularly when the area of coal particle became very small in the late stage of the slag-coal reaction. One of key differences between the CSIRO model (for particle-bubble cell) and that by Story *et al.* (for bulk phase contact) relates the effects of growing bubble size on the relative rates of reactions. Our initial results showed that the increase in the interfacial area between the gas bubble and slag and corresponding decrease in the surface area of char particle could be large enough to shift the rate limiting step from, say, a mixed control to gas-char reaction control. Thus, highlighting the importance of reactivity of char with gaseous species.

Modelling the top-space reactions—post combustion and gas-splash reaction

In the bath smelting reduction process, the majority of the energy is provided by the post combustion of CO and H_2 after reduction, primary combustion and devolatilization reactions. For the HIsmelt process, the CO and H_2 are post combusted in the top space where the metal and slag droplets ejected from the bath are oxidized and heated up by the post combusted gas and return the heat back to the bath.

The following top space chemical reactions are considered: post combustion, decarburization of the metal droplets and reoxidation of the metal and the slag droplets:

$$2CO + O_2 = 2CO_2 \quad 2H_2 + O_2 = 2H_2O \qquad [4]$$

$$[C]_{metal} + CO_2 = 2CO \quad [\mathrm{C}] + H_2O = CO + H_2 \qquad [5]$$

$$[Fe]_{metal} + CO_2 = (FeO)_{slag} + CO$$
$$[\mathrm{Fe}] + H_2O = (FeO) + H_2 \qquad [6]$$

$$(FeO)_{slag} + CO_2 = (Fe_2O_3)_{slag} + CO$$
$$(FeO) + H_2O = (Fe_2O_3) + H_2 \qquad [7]$$

The post combustion model under development combines a kinetic model for the gas-droplet reactions and post

combustion with a model for the movement of droplet in the top space. The kinetic model for gas-droplet reaction involves mass transfer in the gas, metal and slag phases and chemical reaction rate at the gas-droplet interface.

The key assumptions of the model are:

- The process is assumed to be steady-state, gas temperature and composition are temporarily constant during the lifetime of a droplet in the top space
- Full reaction of the post combustion oxygen with the gas evolved from the bath was assumed. The subsequent gas-droplet reaction takes place through various mass transfer and reaction steps.

The key phenomena which are modelled are:

- The temperature and composition of the off-gas
- The decarburization rate of the iron droplets and the reoxidation rate of iron and slag droplets in the top space
- The post combustion degree (PCD), heat transfer efficiency (HTE), coal consumption rate.

The PCD and HTE are defined by the following equations:

$$PCD = \left(\%CO_2 + \%H_2O\right) / \left(\%CO_2 + \%CO + \%H_2O + \%H_2\right) \times 100 \quad [8]$$

$$HTE = \left|\left(1 - \left(H_{g,Tg} - H_{g,TM}\right) / H_{PC,TM}\right)\right| \times 100 \quad [9]$$

where $H_{g,Tg}$ and $H_{g,\,TM}$ are the sensible heats of the off-gas at the gas and melt temperatures, respectively. $H_{PC,\,TM}$ is the enthalpy of post combustion at the melt temperature.

The published pilot plant data of the old version HIsmelt process (horizontal furnace)[34], summarized in Table I, was used to provide some basis for model validation. During the calculation, the flow rate of air for post combustion was varied with the $2O_2/(CO+H_2)$ ratio changing from 0 to 1, while all the other parameters were kept constant as set out in Table I. The variations of HTE, off-gas temperature and PCD with the $O_2/(CO+H_2)$ ratio in the gas, before the post combustion was obtained. The calculated results show that the off-gas temperature, the decarburization rate of iron droplets as well as the reoxidation rate of iron and slag droplets increased with increasing PCD. Figure 11 shows that the HTE decreases with increasing post combustion degree. That is because increasing PCD would increase the off-gas temperature, which results in the increase of the $(H_{g,Tg}\text{-}H_{g,TM})$ as defined in Equation [9], hence decreases the HTE. As shown in Figure 11, the agreement between the calculated and the plant observed HTE under varied PCD is reasonably good and both DIOS[35] and HIsmelt processes[34] were operated with high heat transfer efficiency, which is over 75%. The high HTE is critical for a process with respect to provide more energy generated by the post combustion to satisfy the endothermic requirement for the rapid reduction reactions.

Coal consumption is an important measure of the energy efficiency of the process. The coal consumption was calculated, as a function of the degree of post combustion, based on the energy balance. Changing the coal input rate during the calculation, the target post combustion degree was determined through varying the flow rate of the air for post combustion to keep the value of heat transferred back to the bath constant. In the calculation, the heat loss was assumed to be a constant value of 780 kW observed in the pilot plant experiment. The relation of coal consumption and the PCD, calculated based on the usage of low volatile coal, is shown in Figure 12 together with pilot plant data on HIsmelt[34] and DIOS[36] processes. It is difficult to make direct comparison of coal consumption in different

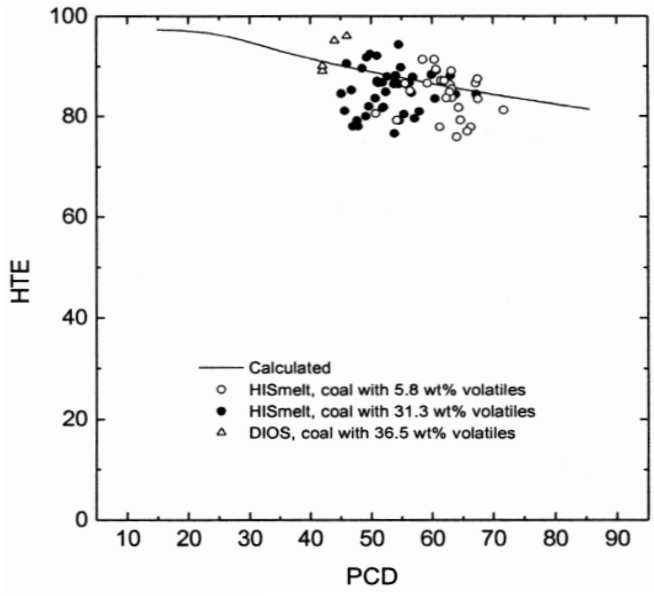

Figure 11. Comparison of the calculated and measured[34–35] heat transfer efficiency as a function of post-combustion degree in HIsmelt and DIOS processes

Table I
Model parameters and the operating data

Hot metal	Production rate	1.5 t/hr	Slag	Basicity	1.5
	Bathe carbon [C]	3 wt%		FeOx	2.8 wt%
	Bath temperature	1746 K		Al_2O_3	17 wt%
	Pressure	1 atm		MgO	3 wt%
Droplets	Generation rate*	40 kg/s	Gas from	CO*	25.96 mole/s
	Slag droplets*	90 wt%	the bath	H_2*	7.44 mole/s
	Metal droplets*	10 wt%		N_2	0.19 mole/s
Parameters			Gas for post	Air	1.715 NM^3/s
Mass	C*	$3.2*10^{-4}$ m/s	Combustion	Temperature	1382 K
Transfer	Slag species*	10^{-5} m/s	Coal	Input rate	1284 kg/hr
coefficient	Gas species*	1 m/s		VM	5.8 wt%
Rate	Gas-slag reactions*	10^{-1} mole/m^{-2}/s		Ash	7.4 wt%
constant	Gas-metal-reactions*	1 mole/m^{-2}/s	Heat loss		780 kW

*estimated

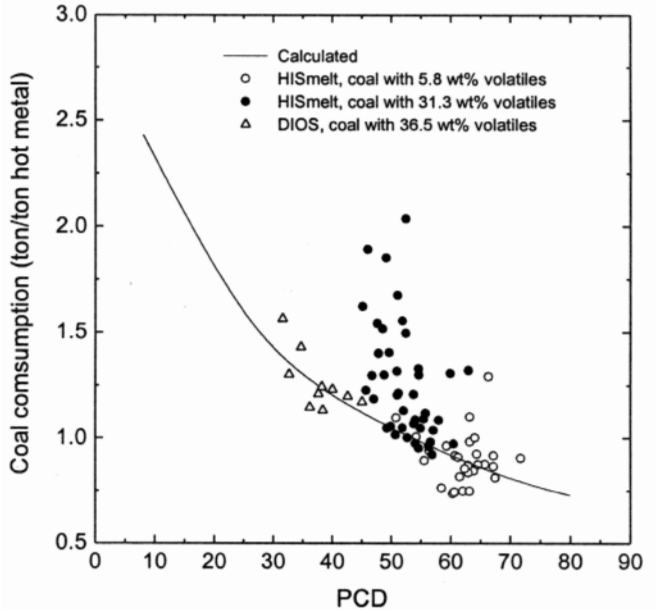

Figure 12. Comparison of the calculated and measured[34,36] coal consumption as a function of post-combustion degree in HIsmelt and DIOS processes

processes as the type of coal (including ash and volatile contents) varied significantly from process to process. However, the trend of coal consumption decreasing with increasing PCD is reflected by the calculation. The predicted behaviour for low volatile coal is in agreement with the measurements for low volatile coal(s) in the HIsmelt reactor at high post-combustion with a steady increase to lower post-combustion degree. Interesting enough the measurements on high volatile coals in the DIOS process at low post-combustion degrees agrees well with the predicted curve. This agreement suggests that in deep slag baths reactors such as DIOS, more efficient heat transfer to the bath from post-combustion could be expected as a result of more intimate contact between the phases. However, one possible drawback from such an intimate contact would be the difficulty in avoiding back oxidation of the bath at high post-combustion degrees. One of the on-going activities at CSIRO is aimed at quantifying the upper limit of post-combustion degree before back oxidation of the bath takes place through the reactions in the plume region.

Concluding remarks

The existing solution models provide good descriptions of thermodynamic behaviour of multi-component metallurgical melts and solid solutions and have been used for analysis of various smelting and refining processes as well as gasification of coals and treatment of wastes. Through linking thermodynamic and transport properties models, the complex behaviour of slags containing suspended solid phases could be predicted. These predictions are in good agreement with measurements made on slags produced by smelting of base metal concentrates in electric furnaces and coal ash slags produced by integrated coal gasifiers, over some orders of magnitude variation in viscosity. Similar agreements have been obtained when results from an electrical conductivity model of slags are compared with experimental data.

Apart from extension of these models to cover kinetics of multi-phase reactions, linkage with the fluid flow and heat transfer models will result in fairly advanced tools for process design and optimization. On-going work on development of such tools has shown some interesting results with respect to the kinetics of coal de-volatilization and combustion of injected coal particles in molten baths as well as the relationships between coal consumption and post-combustion in the top-space of iron bath smelting processes.

Acknowledgements

The authors wish to acknowledge the financial support for part of this work by Anglo Platinum, BHP Steel, Impala Platinum, Kumba Resources, Lonmin Platinum, OneSteel and Rio Tinto through AMIRA International. We also wish to acknowledge financial support by the Australian Government through the former GK Williams Cooperative Research Centre for Extractive Metallurgy, a joint venture between CSIRO Minerals and the University of Melbourne.

References

1. GAYE, H. and WELFRINGER, J. Proc. Second International Symposium on Metallurgical Slags and Fluxes; TMS Warrendale, 1984, pp. 357–375.
2. GAYE, H., GATELLIER, C., and RIBOUD, P.V. Proc. of the Ethem T. Turkdogan Symposium, ISS, 1994, pp. 113–124.
3. GAYE, H., LEHMANN, J., ROCABOIS, R., and RUBY-MEYER, F. Slags modelling and Industrial Application, *Proceeding of the 6th International Conference on Molten slags, fluxes and Salts,* Stockholm, June 2000, CD-ROM.
4. ZHANG, L., JAHANSHAHI, S., SUN, S., LIM, M., BOURKE, B., WRIGHT, S., and SOMERVILLE, M. Development and applications of models for pyrometallurgical processes, *Materials Forum*, 2001, vol. 25, pp. 201–218
5. ZHANG, L., JAHANSHAHI, S., SUN, S., LIM, M., BOURKE, B., WRIGHT, S., and SOMERVILLE M. 'CSIRO's Multiphase Reaction Models and Their Industrial Applications", *JOM*, 2002, vol. 54. no. 11, pp. 51–56.
6. CHEN, C, ZHANG, L., and JAHANSHAHI,S. Review and Thermodynamic Modeling of CoO in Iron Silicate-based Slags and Calcium Ferrite-based Slags; *Proc. of 7th Intl Conference on Molten Slags, Fluxes and Salts*, 2004, Cape Town, South Africa.
7. SOLAR, M.Y., NEAL, R.J., ANTONIONI, T.N., and BELL, M.C. *Journal of Metals*, vol. 31. no. 1, 1979. pp. 26–32.
8. KYLLO, A.K., *M. A. Sc. Thesis,* University of British Columbia, Vancouver, BC, Canada. 1989.
9. ZHOU, D. *Nonferrous Metals*, 1984. no. 4. pp. 4–8.
10. TASKINEN, P., SEPPALA, K., LAULUMAA, J., and POIJARVI, J. *Trans. Instn. Min. Metall.*, vol. 110, 2001. pp. C94–C100.
11. TASKINEN, P., SEPPALA, K., LAULUMAA, J., and POIJARVI, J. *Trans. Instn. Min. Metall.*, vol. 110, 2001. pp. C101–C108.
12. SOMERVILLE, M., ZHANG, L., LIM, M., and JAHANSHAHI, S. Thermodynamic Modelling of Flouride Molten Salts Using the Cell Model; *5th Int. Conference on Molten Slags, Fluxes and Salts*, 1997, Sydney Australia, pp. 629–638.

13. ZHANG, L. and JAHANSHAHI, S. 'Review and Modelling of Viscosity of Silicate Melts: Part I. Viscosity of Binary and Ternary Silicates Containing CaO, MgO and MnO', *Metall. Mater. Trans. B*, 29B, 1998, pp. 177-186.

14. ZHANG, L. and JAHANSHAHI, S. 'Development of Structurally Related Viscosity Model for Silicate Melts', *Proceedings of Sixth International Conference on Molten Salt Chemistry & Technology*, Ed. N. Chen and Z. Qiao, Oct.8–13th, Shanghai, China, 2001. p. 398.

15. WRIGHT, S., ZHANG, L., SUN, S., and JAHANSHAHI, S. 'Viscosities of calcium ferrite and calcium aluminosilicate slags containing spinel particles', *Journal of Non-crystalline solids,* vol. 292, 2001. pp. 15–23.

16. SOMERVILLE, M., WRIGHT, S., SUN, S., and JAHANSHAHI, S. 'Liquidus temperature and viscosity of melter slags'; *Proc. 7th Int. Conference on Molten Slags, Fluxes and Salts*, 2004, Cape Town, South Africa.

17. HURST, H., NOVAK, F., and PATTERSON, J.H. *Fuel*, 1999, vol. .78, pp. 439-44.

18. HURST, H., PATTERSON, J.H., and QUINTANAR, A. *Fuel*, 2000, pp. 1797–9.

19. HURST, H. 'Viscosity data on 15% FeO in fluxed coal ash slags', private communication, 2001, Australia.

20. ZHANG, L., JAHANSHAHI, S., HURST, H., and PATTERSON, J.H. *Eighteenth Annual International Pittsburgh Coal Conference*, Newcastle, Australia, December 4–7, 2001, CD-ROM

21. *Slag Atlas*, 2nd Edition, 1995, Ed: Verein Deutscher Eisenhuttenleutte. Verlag Stahleisen GmbH, D-Dusseldorf, Germany, p. 154.

22. HUNDERMARK, R.J. The electrical conductivity of melter type slags, M.Sc. Dissertation, University of Cape Town, June 2003.

23. ENGELL, H.J. and VYGEN, P. Ionen- und elektronenleitung in CaO-FeO-Fe_2O_3-SiO_2 schmelzen, *Berichte der Bunsengesell fur Physikalische Chemie*, vol. 72, no. 1, 1968. pp. 5–12.

24. FONTANA, A., SEGERS, L., TWITE, K., and WINAND, R. Electrical conductivity of ferrous silicate melts from slag cleaning operations, *TMS-AIME Paper Selection*, Paper no A84-38. 1984.

25. JIAO, Q. and THEMELIS, N.J. Correlations of electrical conductivity to slag composition and temperature, *Metallurgical and Materials Transactions B*, vol. 19B, 1988, pp. 133–140.

26. HUNDERMARK, R.J., JAHANSHAHI, S., and SUN, S. The electrical conductivity of melter type slags, *Proceedings XXII International Mineral Processing Congress*, Cape Town, 2003.

27. FRUEHAN, R.J and OZTURK, B. 'Analysis of bath smelting processes for producing iron', Steel Research, 60, 1989. pp. 129–137.

28. SARMA, B., CRAMB, A.W., and FRUEHAN, R.J. 'Reduction of FeO in Smelting Slags by Solid Carbon: Experimental Results.' *Metall Trans*. 27B, 1996, pp. 717–30.

29. SEO, K. and FRUEHAN, R.J. 'Reduction of FeO in Slag With Coal Char'; *ISIJ International*, vol. 40, no. 1, 2000, pp. 7–15.

30. STORY, S.R. and FRUEHAN, R.J. 'Kinetics of Oxidation of Carbonaceous Materials by CO_2 and H_2O Between 1300 and 1500°C.' *Metall Trans*., vol. 31B, 2000, pp. 43–54.

31. STORY, S.R., SARMA, B., FRUEHAN, R.J., CRAMB, A.W., and BELTON, G.R. 'Reduction of FeO in Smelting Slags by Solid Carbon: Re-Examination of the Influence of the Gas-Carbon Reaction' *Metall Trans, 29B*, 1998, pp. 929–932.

32. CLIFT, R., GRAVE, J.R., and WEBER, M.E. Bubbles, Drops, and Particles, *Academic Press*. New York, NY, 1978.

33. RICHARDS, G.G. and BRIMACOMBE, J.K. 'Kinetics of the Zinc Slag Fuming Process: Part II. Mathematical Model' *Metall Trans*., 16B, 1985, pp. 529–40.

34. KEOGH, J.V., HARDIE, G.J., PHILP, D.K., and BURKE, P.D. *Ironmaking Conference Proceedings*, 1991. pp. 635–649

35. IBARAKI, T., YAMAUCHI, M., SAKAMOTO, Y., HIRATA, H., and KANEMOTO, M. *Iron and Steelmaker*, vol. 22, no. 3. 1995. pp. 83–90.

36. IBARAKI, T., YAMAUCHI, M., MATSUO, M., and KATAYAMA, H. *Iron and Steelmaker*, vol. 22, no. 3. 1995. pp. 91–98.